JOURNAL OF
CHEMICAL &
ENGINEERING
DATA

ARTICLE

pubs.acs.org/jced

Interactions of Volatile Organic Compounds with the Ionic Liquid 1-Butyl-1-methylpyrrolidinium Dicyanamide

Aleš Blahut and Vladimír Dohnal*

Department of Physical Chemistry, Institute of Chemical Technology, 166 28 Prague 6, Czech Republic

S *Supporting Information*

ABSTRACT: Interactions of volatile organic compounds with the ionic liquid (IL) 1-butyl-1-methylpyrrolidinium dicyanamide [BMPYR][DCA] were explored through systematic gas—liquid chromatography retention measurements. Infinite dilution activity coefficients γ_1^∞ and gas—liquid partition coefficients K_L of 30 selected hydrocarbons, alcohols, ketones, ethers, esters, haloalkanes, and nitrogen- or sulfur-containing compounds in [BMPYR][DCA] were determined at five temperatures in the range from (318.15 to 353.15) K. Partial molar excess enthalpies and entropies at infinite dilution were derived from the temperature dependence of the γ_1^∞ values. The linear free energy relationship (LFER) solvation model was used to correlate successfully the K_L values. The LFER correlation parameters and excess thermodynamic functions were analyzed to disclose molecular interactions operating between the IL and the individual solutes. Among other ILs, [BMPYR][DCA] was identified to be a fairly cohesive solvent medium, which is capable of interacting specifically through all modes (lone electron pairs, dipolarity/polarizibility, and hydrogen bonding) with solutes of complementary capabilities. The hydrogen-bond basicity of [BMPYR][DCA] is somewhat lower than that of [EMIM][NO_3] and [EMIM][$MeSO_3$], but in contrast to these latter ILs studied by us previously [BMPYR][DCA] appears to possess also some proton-donating capability. The selectivities of [BMPYR][DCA] for the separation of aromatic hydrocarbons and thiophene from saturated hydrocarbons were found to be only (30 to 70) % of those exhibited by the most selective ILs, as [EMIM][SCN], [EMIM][$MeSO_3$], or [EMIM][NO_3]. On the other hand, the use of [BMPYR][DCA] as an entrainer in extractive distillations of some other mixtures which are difficult to separate (e.g., acetone + methanol) appears to be very promising.

1. INTRODUCTION

During the past decade, ionic liquids (ILs) have been recognized as novel prospective materials for a variety of innovative applications.[1−8] In particular, ILs can offer technologically and environmentally favorable alternatives to common organic solvents in separations of organic substances by means of extraction or extractive distillation. To explore and design such applications, knowledge of interactions of process components with ILs is needed. For screening the interactions of volatile organic compounds (VOCs) as solutes with ILs as solvents the experimental determination of infinite dilution activity coefficients γ_1^∞ by gas—liquid chromatography (GLC) provides an especially convenient and widely accepted approach.[9−15]

In this work, we examine interactions of selected VOCs with the ionic liquid 1-butyl-1-methylpyrrolidinium dicyanamide [BMPYR][DCA].

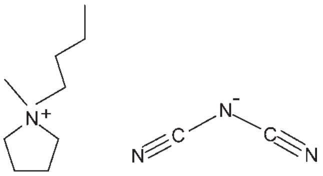

This IL of the third generation with some technologically convenient properties, such as good thermal stability, low viscosity, broad electrochemical window, and high energetic content, may be envisaged to serve for many applications ranging from a powerful solvent[16,17] to a rocket hypergolic propellant.[18] Nevertheless, to our best knowledge, no experimental data on γ_1^∞ in this IL have been reported so far.

The methodology of the present investigation is closely parallel to that we used in our recent studies devoted to 1-ethyl-3-methylimidazolium nitrate,[19] 1-ethyl-3-methylimidazolium methanesulfonate,[20] and 1-ethyl-3-methylimidazolium tetracyanoborate.[21] In this paper, we report thus infinite dilution activity coefficients γ_1^∞ and gas—liquid partition coefficients K_L for the same set of 30 selected hydrocarbons, alcohols, ketones, ethers, esters, haloalkanes, and nitrogen- or sulfur-containing compounds in [BMPYR][DCA] as a function of temperature. The obtained thermodynamic properties are analyzed to disclose the underlying intermolecular interactions governing the observed behavior and to identify the potential of [BMPYR][DCA] to be utilized as an entrainer in solvent-aided separations.

2. THEORY

In gas—liquid chromatography (GLC), the infinite dilution activity coefficient γ_1^∞ and the gas—liquid partition coefficient $K_L = (c_1^L/c_1^G)$ for a solute (1) partitioning between a carrier gas (2) and a nonvolatile liquid solvent (3) are calculated from the solute

Special Issue: Kenneth N. Marsh Festschrift

Received: July 29, 2011
Accepted: October 4, 2011
Published: October 20, 2011

retention according to the following equations[22]

$$\ln \gamma_1^{\infty} = \ln\left(\frac{RTm_3}{V_N p_1^s M_3}\right) - \left[\frac{(B_{11} - v_1^L)p_1^s}{RT}\right] + \left[\frac{(2B_{12} - \bar{v}_1^{\infty})J_3^4 p_0}{RT}\right] \qquad (1)$$

$$\ln K_L = \ln\left(\frac{V_N \rho_3}{m_3}\right) - \left[\frac{(2B_{12} - \bar{v}_1^{\infty})J_3^4 p_0}{RT}\right] \qquad (2)$$

where T is the temperature of the column, m_3, M_3, and ρ_3 the mass, molar mass, and density of the solvent, respectively, and p_1^s the saturated vapor pressure of the solute. The first term on the right-hand side of eqs 1 and 2 is of the principal importance for the calculation of γ_1^{∞} and K_L, respectively, while the remaining terms represent relatively small corrections for gas-phase nonideality. In these corrective terms B_{11} stands for the second virial coefficient of the pure solute, B_{12} for the second cross virial coefficient for the solute−carrier gas interaction, v_1^L for the molar volume of the pure liquid solute, $\bar{v}_1^{\infty}$ for the partial molar volume of the solute at infinite dilution in component 3, and p_0 for the column outlet pressure. The net retention volume V_N is calculated from the following equation

$$V_N = J_3^2 F(t_R - t_D) \qquad (3)$$

where t_R is the retention time of a given solute, t_D the retention time of the nonretainable component, and F the carrier gas flow at the column temperature and column outlet pressure. The corrections J_n^m used in eqs 1 to 3 account for compressibility of the mobile phase and are defined as[22]

$$J_n^m = \frac{n}{m}\left[\frac{(p_i/p_0)^m - 1}{(p_i/p_0)^n - 1}\right] \qquad (4)$$

where p_i stands for the column inlet pressure.

If the infinite dilution activity coefficient is determined as a function of temperature, $\ln \gamma_1^{\infty}$ can be split to its respective enthalpy and entropy components

$$\ln \gamma_1^{\infty} = \frac{\bar{H}_1^{E,\infty}}{RT} - \frac{\bar{S}_1^{E,\infty}}{R} \qquad (5)$$

Assuming that the temperature dependence follows a linear van't Hoff plot

$$\ln \gamma_1^{\infty} = a/T + b \qquad (6)$$

the partial molar excess enthalpy $\bar{H}_1^{E,\infty} = Ra$ and entropy $\bar{S}_1^{E,\infty} = -Rb$ at infinite dilution can be obtained from its slope and intercept, respectively.

3. EXPERIMENTAL SECTION

3.1. Materials. The ionic liquid 1-butyl-1-methylpyrrolidinium dicyanamide ([BMPYR][DCA], M = 208.30 g·mol^{-1}) was obtained in the high purity grade from Merck. Its purity according to the producer's specification was >0.99, the certified water content being <100 ppm (mass basis). The sample was handled with special precautions to avoid any contact with moisture. It was pretreated by prolonged stripping with dry nitrogen to elute volatile impurities. The efficiency of this treatment was checked by gas chromatographic analysis of the outlet gas. The IL samples contained in the GLC columns used for retention measurements underwent further drying in situ during the column conditioning. As determined by Karl Fischer titration, the residual water contents of these samples were below 90 ppm (mass basis).

Inerton Super (Lachema, Czech Republic) of (0.125 to 0.160) mm granularity was used as a solid support for IL in the GLC column. This high-quality, AW-DMCS diatomaceous solid support is characterized by an extreme catalytic and adsorption inertness and a very low specific surface area ((0.3 to 0.55) m^2·g^{-1}).[23] Dichloromethane (Penta, Czech Rep.) used as a solvent in the coating process was of p.a. purity grade, the certified relative water content being ≤ 0.0002 (mass basis). It was dried with molecular sieves prior to use to further decrease its water content. The VOC used as solutes were all of analar purity grade. The solute purity need not to be regarded as critical as gas chromatography itself is a separation method, and thus it can be well assumed that any solute impurities that would possibly affect the measured retention are separated in the course of the chromatographic process. Moreover, since our GLC experiments are carried out at conditions of infinite dilution, individual solute species behave independently. Thus, for convenience, solutes can be injected even in mixtures. Nitrogen (4.0) served as the carrier gas. Its mole fraction purity was 0.9999 with a water content lower than 30 ppm. It was further dried by passing through an Agilent molecular sieve moisture trap MT-400-2 having a guaranteed effluent water content lower than 14 ppb.

3.2. Apparatus. The GLC retention measurements were performed on a computer controlled model 6890 Plus Agilent gas chromatograph (Agilent Technologies, USA) equipped with a flame ionization detector (FID). Stainless steel packed columns with an outer diameter of 1/4 in (wall thickness 1 mm) and three lengths of 0.65 m, 1.2 m, and 1.7 m were used. Solute samples were injected by a 7683 Series Agilent AutoInjector. The signal from the gas chromatographs was recorded and processed by a PC with the ChemStation software (Agilent Technologies, USA).

The liquid density of [BMPYR][DCA], needed to calculate K_L values, was measured with an Anton Paar model DMA 5000 vibrating-tube densimeter applying an automatic built-in correction for viscosity effect. The instrument was duly calibrated by water and nitrogen as recommended by the producer. The repeatability of the density measurement was within 2·10^{-6} g·cm^{-3}. The combined standard uncertainty of the reported density values was estimated to be 1·10^{-4} g·cm^{-3}.

3.3. Column Preparation. All manipulations during the column preparation (including weighing) were performed in a glovebox under dry nitrogen atmosphere. As an initial step, the solid support was loaded with the desired amount of IL. The coating process and determination of IL loading have been described in detail previously.[19] For each batch of the coated support, the value of IL loading λ was established as an average of four determinations, with the relative standard deviation being lower than 1.5 %. The mass of the coated support charged in the column was obtained accurately from differential weighing of the material or the column. Prior to retention measurements, the column installed in the chromatograph was first conditioned by gradual heating up to 363 K under a moderate flow of nitrogen (50 cm^3·min^{-1}) for two days.

3.4. Retention Measurements. Three columns of different lengths loaded with [BMPYR][DCA] (λ being 0.17 and 0.25) were used for retention measurements. The measurements were carried out at several temperatures, namely, 318.15 K, 323.15 K, 333.15 K, 343.15 K, and 353.15 K and nominal flow rates of 10 cm^3·min^{-1} or 50 cm^3·min^{-1} depending on solute retention. At a given temperature, each experiment was replicated three

Table 1. Experimental Density of [BMPYR][DCA]

	$\rho/(\mathrm{g \cdot cm^{-3}})$	
T/K	this work[a]	ref 24
283.15	1.02193	
293.15	1.01626	1.11870
303.15	1.01064	1.11254
313.15	1.00508	1.10644
323.15	0.99956	1.10043
333.15	0.99410	1.09443
343.15	0.98869	1.08852

[a] The equation $\rho/(\mathrm{g \cdot cm^{-3}}) = 1.20449 - 7.19584 \cdot 10^{-4}(T/\mathrm{K}) + 2.64355 \cdot 10^{-7}(T/\mathrm{K})^2$ fits the present data with the standard deviation of $3 \cdot 10^{-6}\ \mathrm{g \cdot cm^{-3}}$.

times in a sequence (during one day) and occasionally also two times during a longer period of time, to check the reproducibility. The precise carrier gas flow rate values were determined with an uncertainty of 0.5 %, using a soap bubble flowmeter placed at the outlet of the column. The outlet pressure p_0 was equal to the atmospheric pressure which was measured using an electronic online barometer with an uncertainty of 0.05 kPa. The pressure drop $(p_i - p_0)$, measured by the chromatograph with an uncertainty of 0.1 kPa, varied between (10 and 50) kPa depending on the carrier gas flow rate, temperature, and length of the column. The temperature of the column controlled by the oven thermostat of the chromatograph was checked against a calibrated platinum resistance thermometer; the uncertainty in the experimental temperature was estimated to 0.2 K.

Solutes were injected into the column as neat substances or in suitable mixtures as vapor (2.5 μL). The uncertainty in determination of the retention time t_R of weakly retained solutes and the retention time of the nonretainable component (methane) t_D was less than 0.01 min. Absolute values of the adjusted retention times $(t_R - t_D)$ varied between (0.5 and 80) min depending on the solute, temperature, carrier gas flow rate, and column used. The relative uncertainty of the adjusted retention time of weakly retained solutes amounted to about (1 to 2) %. As the absolute variation of solute retention was found to increase only slightly with the increasing retention, the relative standard uncertainty of adjusted retention time for appreciably retained solutes did not typically exceed 0.5 %.

4. RESULTS

Infinite dilution activity coefficients and gas−liquid partition coefficients in [BMPYR][DCA] were determined for a set of 30 selected solutes at (318.15, 323.15, 333.15, 343.15, and 353.15) K. Retention measurements were carried out on three columns of lengths 0.65 m, 1.2 m, and 1.7 m loaded with different amounts of the IL, namely, 1.448 g ($\lambda = 0.25$) 1.811 g ($\lambda = 0.17$), and 4.166 g ($\lambda = 0.25$), respectively. The values of γ_1^∞ and K_L were calculated using eqs 1 and 2 from measured solute retention and other data listed in the Supporting Information to ref 19. Partial molar volumes $\bar{v}_1^\infty$ were approximated by the molar volumes of pure liquid solutes v_1^L. The liquid density of [BMPYR][DCA] needed to calculate K_L values was measured in the range from (283.15 to 343.15) K. The results are given in Table 1. The present density data can be adequately represented by quadratic temperature dependence and reliably extrapolated to the highest temperature of our GLC measurements (353.15 K). Listed in Table 1 are for comparison also [BMPYR][DCA] density data recently reported by Sanchez et al.[24] The disparity of the two results is strikingly large, amounting to about 0.1 g·cm^{-3}. Fortunately, two other single density values for this IL are available in the literature, 1.016 g·cm^{-3} at 293.15 K[25] and 1.013 g·cm^{-3} at 298.15 K,[26] that agree very well with values 1.01626 g·cm^{-3} and 1.01345 g·cm^{-3}, respectively, interpolated from our measurements using their smoothing fit. This fact appears to resolve conclusively the issue, thus supporting credibility of our data and indicating that the data reported in ref 24 are those in error.

The values of infinite dilution activity coefficients obtained from measurements on individual columns loaded with different amounts of [BMPYR][DCA] are given in Table S1 in the Supporting Information to this paper. Their mutual correspondence is very good, the γ_1^∞ values being within ± 1.5 % from the mean for the majority of the solutes, and at worst within ± 2 % for solutes with the lowest retention (heptane, octane, diisopropyl ether). Hence, the effects of interfacial adsorption can be considered negligible, and average values can be reported as representative results. The average γ_1^∞ and K_L values obtained from measurements on the different columns are listed in Tables 2 and 3, respectively. Given in these tables are also parameters of respective equations fitting the temperature dependence of the data and the standard deviations of fits. As estimated on the basis of the error propagation law, the combined standard uncertainty of the resulting γ_1^∞ and K_L values in Tables 2 and 3 is within 3 %.

5. DISCUSSION

5.1. Thermodynamic Properties of Solution and Molecular Interactions. As seen from Table 2, the measured γ_1^∞ values exhibit diverse temperature dependences corresponding to both endothermic and exothermic effects accompanying the dissolution of studied solutes in [BMPYR][DCA]. The most pronounced temperature dependences are illustrated in Figures 1 and 2. Table 4 lists the limiting partial molar excess Gibbs energies $\overline{G}_1^{E,\infty} = RT_{ref} \ln \gamma_1^\infty$ of all of the studied solutes in [BMPYR][DCA] at a reference temperature of 323.15 K together with their enthalpy $(\overline{H}_1^{E,\infty})$ and entropy $(T_{ref}\overline{S}_1^{E,\infty})$ contributions, as inferred from the temperature dependence of limiting activity coefficient. The standard uncertainties of the $\overline{H}_1^{E,\infty}$ and $T_{ref}\overline{S}_1^{E,\infty}$ values, estimated taking into account the uncertainties of our γ_1^∞ values and the stability of their fits according to eq 6, are within 0.5 kJ·mol^{-1}.

Some features of the thermodynamic behavior of VOC solutes in [BMPYR][DCA] as apparent from Table 4 are quite similar to those we observed previously[19−21] in [EMIM][NO$_3$], [EMIM][MeSO$_3$], and [EMIM][B(CN)$_4$]. In particular, (i) the largest positive $\overline{G}_1^{E,\infty}$ values are exhibited by aliphatic hydrocarbons; (ii) in the series of hydrocarbons, the solution nonideality then decreases in the sequence: alkanes > alkenes (1-octene) > cycloalkanes > aromatics; (iii) introducing into the solute molecule a polar functionality and even a capability to form with the IL hydrogen bonds further decreases the $\overline{G}_1^{E,\infty}$ down to more or less negative values. The outlined pattern of solution behavior has been observed also for the majority of other ILs and appears to be in general terms understood.[19,20]

A closer comparison of the solution behavior of [BMPYR][DCA] with that of [EMIM][NO$_3$] and [EMIM][MeSO$_3$] shows that the span of observed nonidealities is for [BMPYR][DCA] somewhat narrower than that for the latter two ILs. Note that a similar, but even

Table 2. Experimental Infinite Dilution Activity Coefficients γ_1^∞ of Organic Solutes in [BMPYR][DCA], Constants a and b of Equation 6, and Standard Deviation s of the Fit

	γ_1^∞					a		
solute	318.15 K	323.15 K	333.15 K	343.15 K	353.15 K	K	b	s
heptane	76.0	73.6	68.9	64.7	60.9	713.0	2.091	0.002
octane	115	110	102	95.2	89.2	807.5	2.204	0.001
oct-1-ene	47.3	46.3	44.4	42.4	40.8	476.9	2.359	0.001
cyclohexane	21.1	20.6	19.5	18.5	17.7	566.2	1.272	0.001
methylcyclohexane	32.5	31.7	30.0	28.4	27.1	588.4	1.634	0.001
ethylcyclohexane	50.1	48.4	45.1	42.2	39.6	756.7	1.537	0.002
benzene	1.41	1.42	1.46	1.49	1.53	−268.6	1.185	0.000
toluene	2.17	2.20	2.26	2.30	2.35	−250.3	1.564	0.001
ethylbenzene	3.52	3.55	3.60	3.65	3.69	−154.4	1.744	0.000
m-xylene	3.46	3.50	3.56	3.61	3.67	−182.4	1.816	0.001
methanol	0.344	0.344	0.345	0.347	0.348	−35.0	−0.958	0.000
ethanol	0.550	0.545	0.538	0.530	0.525	149.5	−1.069	0.001
propan-1-ol	0.688	0.680	0.668	0.656	0.647	197.5	−0.996	0.002
propan-2-ol	0.771	0.761	0.746	0.733	0.724	203.7	−0.903	0.002
2,5-dioxahexane	1.19	1.23	1.31	1.39	1.46	−676.8	2.300	0.004
diisopropyl ether	17.9	17.9	18.0	17.9	17.9	−7.2	2.908	0.003
t-butylmethyl ether	6.04	6.13	6.29	6.40	6.53	−246.6	2.576	0.002
tetrahydrofuran	1.36	1.38	1.42	1.46	1.49	−292.9	1.229	0.001
methyl acetate	1.51	1.53	1.56	1.59	1.63	−222.4	1.114	0.002
ethyl acetate	2.33	2.35	2.39	2.43	2.47	−186.0	1.431	0.001
acetone	0.905	0.917	0.942	0.963	0.986	−273.6	0.761	0.001
butanone	1.26	1.27	1.30	1.33	1.35	−230.5	0.955	0.000
dimethyl carbonate	1.26	1.27	1.29	1.31	1.33	−167.7	0.759	0.001
dichloromethane	0.541	0.558	0.591	0.623	0.655	−613.6	1.315	0.001
chloroform	0.391	0.411	0.453	0.496	0.540	−1038.2	2.324	0.001
halothane	0.568	0.606	0.694	0.776	0.866	−1356.8	3.701	0.004
tetrachloromethane	2.04	2.11	2.25	2.38	2.50	−655.1	2.774	0.003
nitromethane	0.592	0.596	0.604	0.609	0.615	−118.9	−0.149	0.001
acetonitrile	0.670	0.676	0.680	0.684	0.687	−77.7	−0.154	0.002
thiophene	0.851	0.868	0.901	0.931	0.962	−392.9	1.074	0.000

more pronounced, reduction of the nonideality span has been also encountered for [EMIM][B(CN)$_4$].[21] The $\overline{G}_1^{E,\infty}$ values for all solutes (except for methanol and ethanol) are in [BMPYR][DCA] consistently smaller (less positive or more negative) than those in [EMIM][NO$_3$] and [EMIM][MeSO$_3$]. The smaller values of $\overline{G}_1^{E,\infty}$and also $\overline{H}_1^{E,\infty}$ for aliphatic hydrocarbons in [BMPYR][DCA] suggest that the cohesivity of this IL is not as extremely high as that of the two other ILs we studied previously.

As seen from Table 4, the thermal effects upon dissolution for aliphatic hydrocarbons and alcohols higher than methanol are in [BMPYR][DCA] positive, while those of other solutes range from effectively zero to considerably negative. The strongly endothermic dissolution of aliphatics stems from the energetic weakness of their interaction with the IL, but the much smaller $\overline{H}_1^{E,\infty}$ values of alcohols result essentially from incomplete compensation of two effects: the endothermic breaking of hydrogen bonds between self-associated alcohol molecules and the exothermic forming of hydrogen bonds between the alcohol molecules and the IL. Like in the case of [EMIM][B(CN)$_4$], the most exothermic dissolution was encountered for 2,5-dioxahexane, halothane, and chloroform and results undoubtedly from hydrogen-bond complex formation between these solutes and the IL solvent. For 2,5-dioxahexane on one hand and halothane and chloroform on the other hand, the mechanism of this hydrogen bonding is however different: while the latter solutes are hydrogen-bond donors, the former is a hydrogen-bond acceptor. The hydrogen-bond basicity of [BMPYR][DCA] is most probably provided by the multiple lone electron pairs of its dicyanamide anion. The source of hydrogen-bond acidity of [BMPYR][DCA] must be the unsubstituted hydrogen atoms on the pyrrolidinium ring of its cation.

For all solutes except alcohols, nitromethane, and acetonitrile, the solution in [BMPYR][DCA], like in [EMIM][B(CN)$_4$], is accompanied with more or less significant entropy losses. This may suggest that solute molecules arrange in the IL structure, following the highly orientational character of involved intermolecular forces. The positive values of $\overline{S}_1^{E,\infty}$ for alcohols result from breaking their hydrogen-bond structures during the solution process. The positive values of $\overline{S}_1^{E,\infty}$ and the negative values of $\overline{G}_1^{E,\infty}$ for nitromethane and acetonitrile, the solutes of the smallest molecular size, appear to be largely of combinatorial origin.

5.2. LFER Solvation Model Correlation and Molecular Interactions.

As in our previous studies, the gas−liquid partitioning data obtained in this work were also correlated using the linear free

Table 3. Experimental Gas−Liquid Partition Coefficients K_L of Organic Solutes in [BMPYR][DCA], Constants a and b of $\ln K_L = a/T + b$, and Standard Deviation s of the Fit

	K_L					a		
solute	318.15 K	323.15 K	333.15 K	343.15 K	353.15 K	K	b	s
heptane	11.1	9.45	7.00	5.32	4.14	3163.8	−7.544	0.007
octane	21.1	17.6	12.5	9.11	6.80	3634.2	−8.379	0.007
oct-1-ene	42.3	34.9	24.2	17.4	12.8	3842.4	−8.337	0.007
cyclohexane	20.5	17.6	13.4	10.4	8.22	2923.6	−6.175	0.005
methylcyclohexane	26.3	22.4	16.6	12.6	9.79	3173.7	−6.710	0.005
ethylcyclohexane	53.9	44.9	31.9	23.3	17.5	3617.3	−7.389	0.007
benzene	308	255	177	127	93.1	3847.3	−6.365	0.005
toluene	597	481	320	220	155	4326.1	−7.211	0.005
ethylbenzene	984	778	500	331	227	4716.9	−7.939	0.006
m-xylene	1136	894	568	374	254	4815.6	−8.106	0.006
methanol	856	697	472	328	234	4163.1	−6.336	0.004
ethanol	1017	815	536	363	253	4469.4	−7.127	0.005
propan-1-ol	2011	1574	988	643	431	4949.8	−7.956	0.005
propan-2-ol	916	727	469	313	215	4656.4	−7.820	0.005
2,5-dioxahexane	469	373	242	163	113	4574.4	−8.234	0.008
diisopropyl ether	16.3	13.8	10.0	7.50	5.75	3353.1	−7.753	0.008
t-butylmethyl ether	30.5	25.7	18.7	14.0	10.7	3356.3	−7.138	0.006
tetrahydrofuran	196	163	115	83.8	62.4	3679.9	−6.292	0.006
methyl acetate	132	110	78.6	57.6	43.1	3591.6	−6.411	0.005
ethyl acetate	180	148	102	72.6	53.0	3927.0	−7.155	0.006
acetone	214	180	129	94.5	71.0	3547.6	−5.787	0.005
butanone	355	292	202	144	105	3915.7	−6.440	0.005
dimethyl carbonate	544	442	298	207	148	4184.9	−6.859	0.006
dichloromethane	204	170	121	88.1	65.7	3633.7	−6.108	0.005
chloroform	576	465	310	213	150	4317.7	−7.219	0.005
halothane	276	222	145	99.1	69.4	4432.2	−8.317	0.009
tetrachloromethane	184	150	102	71.6	51.8	4078.2	−7.608	0.007
nitromethane	1740	1409	943	653	463	4254.1	−5.914	0.005
acetonitrile	709	590	417	302	224	3695.5	−5.055	0.004
thiophene	595	486	331	232	167	4079.3	−6.437	0.005

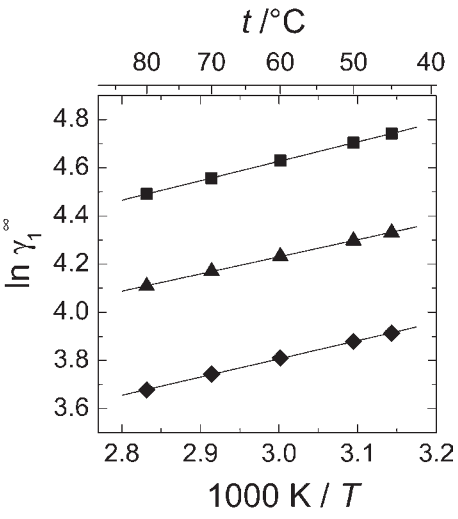

Figure 1. Temperature dependence of the limiting activity coefficient of some solutes with appreciably endothermic dissolution in [BMPYR][DCA]: ■, octane; ▲, heptane; ◆, ethylcyclohexane.

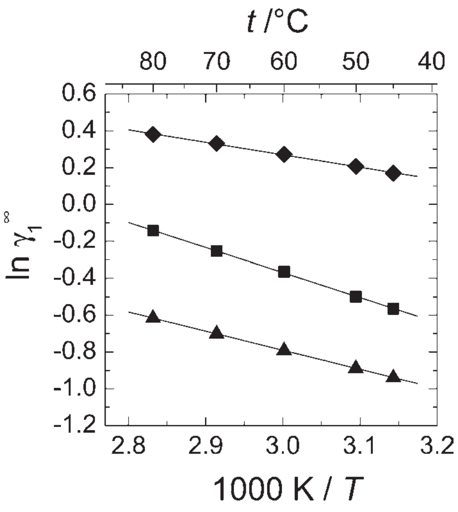

Figure 2. Temperature dependence of the limiting activity coefficient of some solutes with appreciably exothermic dissolution in [BMPYR][DCA]: ■, halothane; ▲, chloroform; ◆, 2,5-dioxahexane.

energy relationship (LFER) solvation model of Abraham.[27,28] This simple model has been shown[13,29−33] to provide a powerful tool for analyzing the contributions of individual intermolecular interactions to the gas−liquid partitioning process and particularly for characterizing solvation properties of ILs. The LFER equation was used in the form

$$\log K_L = c + eE + sS + aA + bB + lL \tag{7}$$

where the capital letters (E, S, A, B, L) are the solute descriptors and the lower case letters (e, s, a, b, l) are the system constants representing respective contributions from the solvent. The c term is the model constant. The solute descriptors are: E the excess molar refraction (solute tendency to interact through lone electron pairs), S the solute dipolarity/polarizibility, A the solute effective hydrogen bond acidity, B the solute hydrogen bond basicity, L the logarithm of the gas−hexadecane partition coefficient (298 K). The L descriptor involves the contributions of solute to the solvent cavity formation and the solute−solvent dispersion interactions. The Abraham's solute descriptors are available for a large number of compounds[27,34] and for those studied in this work were listed in Supporting Information to ref 19. The system constants can be calculated from experimental K_L values for a set of solutes using standard procedures of multiple regression analysis. Provided the solute set is sufficiently representative from the chemical and statistical point of view, the calculated system constants are not mere correlation parameters but have physical significance, their magnitudes indicating the relative importance of individual intermolecular interactions for a given solvent (ionic liquid).

The system constants calculated for [BMPYR][DCA] at 323.15 K are listed together with some statistical characteristics of the fit in Table 5. Values of the coefficient of determination, standard deviation of fit, Fischer F-statistics, and the standard deviations of the individual system constants indicate consistently that the fitting results are statistically sound. The very good performance of the LFER solvation model is graphically illustrated in Figures 3 and 4. Furthermore, as seen from Table 5, the values of system parameters are virtually unaffected when some correlation outliers are excluded. This fact means that the correlation is sufficiently robust and can be considered as truly representative. A noteworthy finding is that the identified outliers (halothane, dimethyl carbonate) are the same as those in our previous studies,[19−21] suggesting thus that their descriptors may not be appropriate.

Table 4. Limiting Partial Molar Excess Gibbs Energies $\overline{G}_1^{E,\infty}$, Enthalpies $\overline{H}_1^{E,\infty}$, and Entropies $T_{ref}\overline{S}_1^{E,\infty}$ of Organic Solutes in [BMPYR][DCA] at a Reference Temperature T_{ref} = 323.15 K

	$\overline{G}_1^{E,\infty}$	$\overline{H}_1^{E,\infty}$	$T_{ref}\overline{S}_1^{E,\infty}$
solute	kJ·mol^{-1}	kJ·mol^{-1}	kJ·mol^{-1}
heptane	11.5	5.9	−5.6
octane	12.6	6.7	−5.9
oct-1-ene	10.3	4.0	−6.3
cyclohexane	8.1	4.7	−3.4
methylcyclohexane	9.3	4.9	−4.4
ethylcyclohexane	10.4	6.3	−4.1
benzene	0.9	−2.2	−3.2
toluene	2.1	−2.1	−4.2
ethylbenzene	3.4	−1.3	−4.7
m-xylene	3.4	−1.5	−4.9
methanol	−2.9	−0.3	2.6
ethanol	−1.6	1.2	2.9
propan-1-ol	−1.0	1.6	2.7
propan-2-ol	−0.7	1.7	2.4
2,5-dioxahexane	0.6	−5.6	−6.2
diisopropyl ether	7.8	−0.1	−7.8
t-butylmethyl ether	4.9	−2.1	−6.9
tetrahydrofuran	0.9	−2.4	−3.3
methyl acetate	1.1	−1.8	−3.0
ethyl acetate	2.3	−1.5	−3.8
acetone	−0.2	−2.3	−2.0
butanone	0.6	−1.9	−2.6
dimethyl carbonate	0.6	−1.4	−2.0
dichloromethane	−1.6	−5.1	−3.5
chloroform	−2.4	−8.6	−6.2
halothane	−1.3	−11.3	−9.9
tetrachloromethane	2.0	−5.4	−7.5
nitromethane	−1.4	−1.0	0.4
acetonitrile	−1.1	−0.6	0.4
thiophene	−0.4	−3.3	−2.9

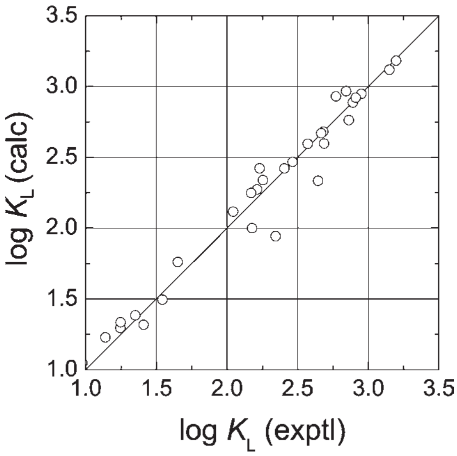

Figure 3. Calculated vs experimental logarithmic gas−liquid partition coefficients log K_L for 30 solutes in [BMPYR][DCA] at 323.15 K using the LFER solvation model.

Table 5. LFER System Constants for [BMPYR][DCA] at 323.15 K

	system constants[a]						statistics[b]			
set of solutes	e	s	a	b	l	c	R^2	SD	F	n
complete	0.51 (0.20)	2.33 (0.19)	3.96 (0.33)	0.26 (0.16)	0.49 (0.07)	−0.50 (0.24)	0.963	0.138	124	30
outliers excluded[c]	0.71 (0.12)	2.23 (0.11)	3.96 (0.20)	0.43 (0.10)	0.51 (0.04)	−0.64 (0.15)	0.988	0.082	357	28

[a] Values in parentheses are the standard uncertainties of the parameters. [b] R^2, coefficient of determination; SD, standard deviation of fit; F, Fischer's statistics; n, number of solutes. [c] Outliers: halothane, dimethyl carbonate.

Considering the magnitudes of its system constants, [BMPYR][DCA] can be classified as a fairly cohesive IL which possesses a distinct capacity for participating in lone electron pair interactions, dipole-type interactions, and hydrogen-bonding type interactions with solutes of complementary capabilities. To put this into the perspective with other solvents, values of system constants for [EMIM][NO_3], [EMIM][$MeSO_3$], and [EMIM][$B(CN)_4$] that we studied previously, and for two other ILs and three molecular solvents as obtained by Poole,[13] are compared in Table 6 with those for [BMPYR][DCA] at 354 K (Poole's experimental temperature). The solvent cohesion as an opposing factor to the solute solvation can be relatively assessed by the compound term ($c + lL$).[29] For the solvents considered and octane as a probe solute, this term is given in Table 7. The solvents in Table 7 are listed in the order of the decreasing ($c + lL$) term, that is, in the order of their increasing cohesion. This scale suggests that [BMPYR][DCA] is appreciably more cohesive than most common molecular GC stationary phases and some ILs, but among ILs its cohesivity does not definitely belong to the highest. Indeed, when we compare the cohesive energy density inferred from recent experimental determinations of vaporization enthalpies of some ILs,[35−37] we find that its value for [BMPYR][DCA] (807 MPa) is about 85 % of that for [EMIM][BF_4] (947 MPa) and only about 70 % of that for [EMIM][NO_3] (1129 MPa). On the other hand, its cohesive energy density is substantially higher than that of [EMIM][$B(CN)_4$] (619 MPa). As seen from Table 6, [BMPYR][DCA] exhibits considerable abilities to interact with lone electron pairs (system constant e) and to accept hydrogen bonds (system constant a) which approach those of [EMIM][NO_3] and [EMIM][$MeSO_3$]. Its ability for dipolarity/polarizability interactions (system constant s), being close to that of 1,2,3-tris(2-cyanoethoxy)propane (one of the most polar GC stationary phases) and of [EMIM][$B(CN)_4$], is strong, but as not extreme as for [EMIM][NO_3] and [EMIM][$MeSO_3$]. Unlike the latter ILs, [BMPYR][DCA] shows also some proton-donating capability (system constant b). Although weaker than for [EMIM][$B(CN)_4$], this capability is undisputable. As we have indicated recently,[21] [EMIM][NO_3] and [EMIM][$MeSO_3$] lack the proton-donating capability because the acidic hydrogens (in particular that in position 2) on their [EMIM] rings are blocked, being engaged in interactions with the hard counteranions.

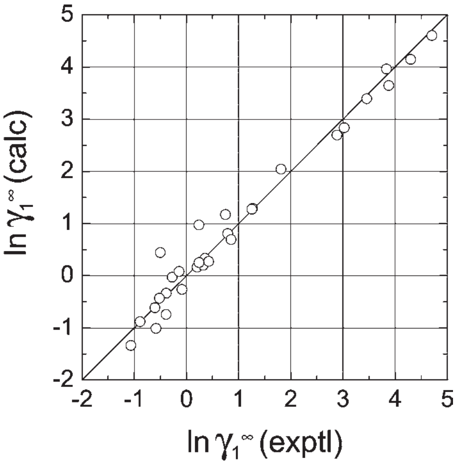

Figure 4. Calculated vs experimental logarithmic infinite dilution activity coefficients ln γ_1^∞ for 30 solutes in [BMPYR][DCA] at 323.15 K using the LFER solvation model.

5.3. Separation Performance of [BMPYR][DCA]. The potential for utilization of solvents in separation processes can be

Table 7. Contribution of Solvent Cavity Formation and Solute−Solvent Dispersion Interactions to log K_L of Octane at 354 K

solvent	$c + lL$
squalane	2.49
Carbowax 20 M	1.53
1-ethyl-3-methylimidazolium tetracyanoborate	1.07
butylammonium thiocyanate	0.90
1,2,3-tris(2-cyanoethoxy)propane	0.84
1-butyl-1-methylpyrrolidinium dicyanamide	0.82
1-ethyl-3-methylimidazolium nitrate	0.10
1-ethyl-3-methylimidazolium methanesulfonate	0.04
ethylammonium nitrate	−0.10

Table 6. Comparison of LFER System Constants for Several Liquids at 354 K[a]

	system constants[b]						statistics[c]			
solvents	e	s	a	b	l	c	R^2	SD	F	n
			Molecular Liquids							
squalane	0.07 (0.03)	0	0	0	0.73 (0.01)	−0.19 (0.02)	0.998	0.025	7638	22
Carbowax 20 M	0.27 (0.08)	1.52 (0.07)	2.16 (0.13)	0	0.53 (0.02)	−0.42 (0.10)	0.988	0.053	311	21
1,2,3-tris(2-cyanoethoxy)propane	0.29 (0.10)	2.17(0.10)	1.99 (0.18)	0.28 (0.11)	0.36 (0.02)	−0.48 (0.12)	0.986	0.062	213	22
			Ionic Liquids							
butylammonium thiocyanate	0.14 (0.09)	1.65 (0.09)	2.76 (0.16)	1.32 (0.11)	0.45 (0.02)	−0.75 (0.10)	0.990	0.058	326	23
1-ethyl-3-methylimidazolium tetracyanoborate	0.24 (0.09)	2.15 (0.08)	2.04 (0.14)	0.61 (0.07)	0.46 (0.03)	−0.64 (0.11)	0.990	0.059	432	28
ethylammonium nitrate	0.47 (0.16)	2.21 (0.16)	3.38 (0.28)	1.03 (0.17)	0.21 (0.04)	−0.87 (0.20)	0.988	0.089	175	17
1-butyl-1-methylpyrrolidinium dicyanamide	0.70 (0.10)	2.03 (0.09)	3.43 (0.16)	0.33 (0.08)	0.41 (0.04)	−0.68 (0.12)	0.991	0.066	462	28
1-ethyl-3-methylimidazolium nitrate	0.83 (0.14)	2.50 (0.14)	3.78 (0.26)	0	0.24 (0.06)	−0.78 (0.20)	0.983	0.109	327	27
1-ethyl-3-methylimidazolium methanesulfonate	0.87 (0.13)	2.42 (0.13)	4.51 (0.24)	0	0.20 (0.06)	−0.69 (0.18)	0.988	0.103	467	28

[a] Results for [BMPYR][DCA] are from this work, for [EMIM][NO_3], [EMIM][$MeSO_3$], and [EMIM][$B(CN)_4$] from refs 19−21 respectively, for all other solvents from ref 13. [b] Values in parentheses are the standard uncertainties of the parameters. [c] R^2, coefficient of determination; SD, standard deviation of fit; F, Fischer's statistics; n, number of solutes.

Table 8. Selectivities S_{12}^{∞} and Capacities κ_2^{∞} of Some [BMPYR]- or [EMIM]-Based Ionic Liquids and Molecular Solvents for Four Separation Pairs at 323.15 K

	S_{12}^{∞}							
	cyclohexane (1)	heptane (1)	cyclohexane (1)	heptane (1)	κ_2^{∞}			
solvent	benzene (2)	toluene (2)	thiophene (2)	thiophene (2)	benzene	toluene	thiophene	ref
[EMIM][SCN]	25.7	62.6			0.29	0.16		38
[EMIM][$MeSO_3$]	25.6	63.6	55.8	289	0.22	0.11	0.49	20
[EMIM][NO_3]	23.8	48.5	82.3	307	0.20	0.11	0.71	19
[BMPYR][SCN]	18.4	44.6	31.9	127	0.53	0.32	0.91	39
[EMIM][DCA]	18.0	42.4	29.1	114	0.38	0.23	0.62	40
[BMPYR][DCA]	14.5	33.4	23.7	84.8	0.70	0.45	1.15	this work
[BMPYR][CF_3SO_3]	13.9	25.4	19.1	53.1	0.68	0.45	0.94	41
[BMPYR][NTf_2]	9.0				1.14			42
[BMPYR][$B(CN)_4$]	8.6	16.8	10.5	27.9	1.18	0.87	1.44	43
sulfolane	11.0	19.5	16.3	45.1	0.43	0.27	0.63	44[a]
N-methyl-2-pyrrolidinone (NMP)	6.5	9.5	9.0	16.6	0.88	0.70	1.22	44[a]

[a] Values given are based on a comprehensive critical compilation of available γ^{∞} literature data and their temperature dependence fit.

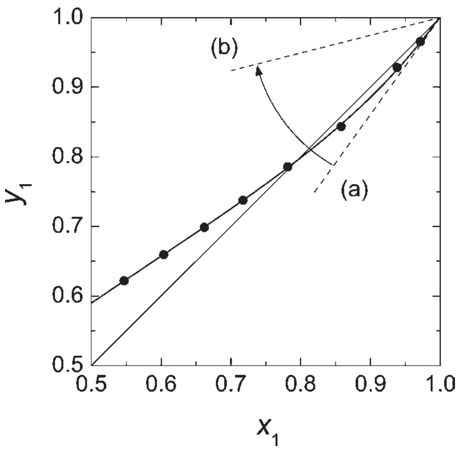

Figure 5. Effect of [BMPYR][DCA] on the terminal slope of the $y_1(x_1)$ curve at $x_1 = 1$ for the acetone(1)−methanol(2) system at 323.15 K: (a) terminal slope for the IL-free system, ●, experimental VLE data from ref 45; (b) terminal slope for the limiting situation when the components to be separated are at infinite dilution in [BMPYR][DCA], based on experimental data from this work (Table 9).

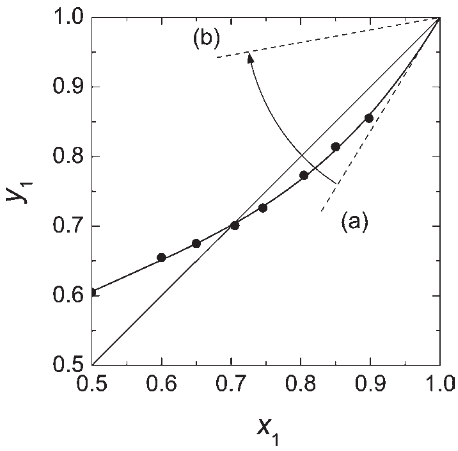

Figure 6. Effect of [BMPYR][DCA] on the terminal slope of the $y_1(x_1)$ curve at $x_1 = 1$ for the ethyl acetate(1)−ethanol(2) system at 323.15 K: (a) terminal slope for the IL-free system, ●, experimental VLE data from ref 46; (b) terminal slope for the limiting situation when the components to be separated are at infinite dilution in [BMPYR][DCA], based on experimental data from this work (Table 9).

assessed in terms of their selectivities $S_{12}^{\infty} = \gamma_1^{\infty}/\gamma_2^{\infty}$ and capacities $\kappa_2^{\infty} = 1/\gamma_2^{\infty}$ as derived from the limiting activity coefficient values of the components to be separated in these solvents. For [BMPYR][DCA], together with some other [BMPYR]- or [EMIM]-based ILs and two well-established molecular separating agents, the values of S_{12}^{∞} and κ_2^{∞} at 323.15 K are listed in Table 8 for the four petrochemical model separation pairs cyclohexane(1)−benzene(2), heptane(1)−toluene(2), cyclohexane(1)−thiophene(2), and heptane(1)−thiophene(2).

As seen in Table 8, the selectivity values S_{12}^{∞} of [BMPYR][DCA] for these mixtures are quite high. They are significantly higher than those of the classical molecular separating agents, but not attaining the values of the most selective [EMIM] ILs. Among the five [BMPYR] ILs studied so far, [BMPYR][DCA] ranks second after [BMPYR][SCN]. The value of the solvent selectivity provides an indication of feasibility and/or efficiency of a given solvent-aided separation. For the economy of large-scale industrial separations, the solvent capacity for the component to be extracted, κ_2^{∞}, is however a parameter of at least the same importance as S_{12}^{∞}. The value of κ_2^{∞} determines the amount of the solvent needed and, in turn, greatly affects the investment and operating costs of the entire separation plant. Thus, for a separation process to be economical, the value of κ_2^{∞} must be sufficiently high. Since κ_2^{∞} generally tends to decrease with S_{12}^{∞}, then in practice some compromise between S_{12}^{∞} and κ_2^{∞} provides often the right choice. In this respect, [BMPYR][DCA] might be a good separation agent candidate, because it offers much higher capacities than the most selective ILs do, while keeping its selectivity also appropriately high. Comparing [BMPYR][DCA] to sulfolane, it is seen that this IL surpasses it significantly in both of these parameters.

It is to be noted that [BMPYR][DCA] can be used as an efficient entrainer in extractive distillations of some other mixtures which are

Table 9. Selectivity S^{∞}_{12}, Separation Factor $\alpha^{\infty}_{12(\text{in IL})}$, and Capacity κ^{∞}_{2} of [BMPYR][DCA] for Two Azeotropic Separation Pairs at 323.15 K

separation pair	S^{∞}_{12}	$\alpha^{\infty}_{12(\text{inIL})}$	κ^{∞}_{2}
acetone(1)−methanol(2)	2.66	3.93	2.90
ethyl acetate(1)−ethanol(2)	4.32	5.55	1.83

difficult to separate. To demonstrate this, we give two examples of industrially important azeotropic systems, acetone(1)−methanol(2) and ethyl acetate(1)−ethanol(2), whose y_1−x_1 diagrams at 323.15 K are shown in Figures 5 and 6, respectively. Marked in these diagrams and denoted as (a) are respective terminal slopes of $y_1(x_1)$ curves at $x_1 = 1$. Obviously, the corresponding separation factors (i.e., the relative volatility of lower boiling components, acetone, and ethyl acetate) α_{12} at $x_1 = 1$ are smaller than unity, reflecting thus the azeotropic behavior of these systems. Adding [BMPYR][DCA] to these systems as a third component moves the slopes in the direction indicated by arrows, increasing thus the separation factors above unity, that is, breaking the azeotropes. The other terminal slopes denoted as (b) correspond to the limiting situation when the components to be separated are at infinite dilution in the IL, the respective separation factor being

$$\alpha^{\infty}_{12(\text{in IL})} = \left(\frac{y_1/x_1}{y_2/x_2}\right)^{\infty} = \frac{\gamma_1^{\infty} p_1^{\text{s}}}{\gamma_2^{\infty} p_2^{\text{s}}} = S^{\infty}_{12}\frac{p_1^{\text{s}}}{p_2^{\text{s}}} \qquad (8)$$

Numerical data on S^{∞}_{12}, κ^{∞}_{2}, and $\alpha^{\infty}_{12(\text{in IL})}$ for these two systems are given in Table 9. These favorable values as well as their impact on the y_1−x_1 diagrams illustrated in Figures 5 and 6 evidence the efficiency and practical convenience of [BMPYR][DCA] as an entrainer whose more or less minute contents should ensure azeotrope breaking and effective separation of these mixtures.

6. CONCLUSIONS

In this work, we have examined interactions of various types of organic solutes with the ionic liquid [BMPYR][DCA] through methodical GLC retention measurements. Infinite dilution activity coefficients and gas−liquid partition coefficients of 30 hydrocarbons, alcohols, ketones, ethers, esters, haloalkanes, and nitrogen- or sulfur-containing VOCs in [BMPYR][DCA] have been determined over a range of temperatures, which allowed derivation of respective enthalpic and entropic contributions.

The analysis of the obtained thermodynamic properties and their interpretation in terms of the LFER solvation model have identified [BMPYR][DCA] as a fairly cohesive IL, yet its cohesivity is distinctly lower than that for the most cohesive [EMIM] ILs with [SCN], [MeSO_3], or [NO_3] anions. Compared to [EMIM][NO_3] and [EMIM][MeSO_3] we studied previously, this IL interacts somewhat less strongly through lone electron pairs and dipolarity/polarizibility with solutes of complementary capabilities. Contrary to [EMIM][NO_3] and [EMIM][MeSO_3] which lack the proton-donating ability, this IL acts as both proton acceptor and proton donor. Its hydrogen bond acidity, unambiguously associated with the [BMPYR] cation, is however, in comparison to its hydrogen bond basicity, rather weak.

As a solvent for the separation of aromatic hydrocarbons and thiophene from aliphatics, [BMPYR][DCA] offers a separation selectivity that is considerably less than that of the most powerful [EMIM]-based ILs, but its capacity to extract aromatics and thiophene from such mixtures is much larger. We have also shown that [BMPYR][DCA] could serve as an efficient entrainer in separations of other nonpetrochemical azeotropic systems of industrial importance by extractive distillation.

■ ASSOCIATED CONTENT

Ⓢ Supporting Information. Experimental infinite dilution activity coefficients γ_1^{∞} of 30 organic solutes in [BMPYR][DCA] obtained using three different columns. This material is available free of charge via the Internet at http://pubs.acs.org.

■ AUTHOR INFORMATION

Corresponding Author

*E-mail: dohnalv@vscht.cz. Address for correspondence: Dr. Vladimír Dohnal, Department of Physical Chemistry, Institute of Chemical Technology, Technická 5, 166 28 Prague 6, Czech Republic. Tel.: +420 220 444 297.

Funding Sources

This work was funded from Ministry of Education of the Czech Republic (Grant No. MSM 604 613 7307).

■ REFERENCES

(1) Wasserscheid, P.; Keim, W. Ionic Liquids - New “Solutions” for Transition Metal Catalysis. *Angew. Chem., Int. Ed.* **2000**, *39*, 3772–3789.

(2) Rogers, R. D.; Seddon, K. R. *Ionic Liquids: Industrial Applications to Green Chemistry*; ACS Symposium Series 818; American Chemical Society: Washington, DC, 2002.

(3) Rogers, R. D.; Seddon, K. R. *Ionic Liquids as Green Solvents: Progress and Prospects*; ACS Symposium Series 856; American Chemical Society: Washington, DC, 2003.

(4) Rogers, R. D.; Seddon, K. R. *Ionic Liquids IIIA: Properties and Structure*; ACS Symposium Series 901; American Chemical Society: Washington, DC, 2005.

(5) Rogers, R. D.; Seddon, K. R. *Ionic Liquids IIIB. Fundamentals, Progress, Challenges, and Opportunities. Transformations and Processes*; ACS Symposium Series 915; American Chemical Society: Washington, DC, 2005.

(6) Brennecke, J. F.; Rogers, R. D. Seddon, K. R. *Ionic Liquids IV. Not Just Solvents Anymore*; ACS Symposium Series 975; American Chemical Society: Washington, DC, 2007.

(7) Plechkova, N. V.; Rogers, R. D. Seddon, K. R. *Ionic Liquids: from Knowledge to Application*; ACS Symposium Series 1030; American Chemical Society: Washington, DC, 2009.

(8) Malhotra, S. V. *Ionic Liquid Applications: Pharmaceuticals, Therapeutics, and Biotechnology*; ACS Symposium Series 1038; American Chemical Society: Washington, DC, 2010.

(9) Arancibia, E. L.; Castells, R. C.; Nardillo, A. M. Thermodynamic study of the behaviour of two molten organic salts as stationary phases in gas chromatography. *J. Chromatogr.* **1987**, *398*, 21–29.

(10) Heintz, A.; Kulikov, D. V.; Verevkin, S. P. Thermodynamic properties of mixtures containing ionic liquids. 1. Activity coefficients at infinite dilution of alkanes, alkenes, and alkylbenzenes in 4-methyl-N-butylpyridinium tetrafluoroborate using gas-liquid chromatography. *J. Chem. Eng. Data* **2001**, *46*, 1526–1529.

(11) Letcher, T. M.; Soko, B.; Ramjugernath, D.; Deenadayalu, N.; Nevines, A.; Naicker, P. K. Activity coefficients at infinite dilution of organic solutes in 1-hexyl-3-methylimidazolium hexafluorophosphate from gas-liquid chromatography. *J. Chem. Eng. Data* **2003**, *48*, 708–711.

(12) Kato, R.; Gmehling, J. Activity coefficients at infinite dilution of various solutes in the ionic liquids $[\text{MMIM}]^+[\text{CH}_3\text{SO}_4]^-$, $[\text{MMIM}]^+[\text{CH}_3\text{OC}_2\text{H}_4\text{SO}_4]^-$, $[\text{MMIM}]^+[(\text{CH}_3)_2\text{PO}_4]^-$, $[\text{C}_5\text{H}_5\text{NC}_2\text{H}_5]^+[(\text{CF}_3\text{SO}_2)_2\text{N}]^-$ and $[\text{C}_5\text{H}_5\text{NH}]^+$ $[\text{C}_2\text{H}_5\text{OC}_2\text{H}_4\text{OSO}_3]^-$. *Fluid Phase Equilib.* **2004**, *226*, 37–44.

(13) Poole, C. F. Chromatographic and spectroscopic methods for the determination of solvent properties of room temperature ionic liquids. *J. Chromatogr., A* **2004**, *1037*, 49–82.

(14) Mutelet, F.; Butet, V.; Jaubert, J.-N. Application of Inverse Gas Chromatography and Regular Solution Theory for Characterization of Ionic Liquids. *Ind. Eng. Chem. Res.* **2005**, *44*, 4120–4127.

(15) Dohnal, V. Measurement of Limiting Activity Coefficients Using Analytical Tools. In *Measurement of the Thermodynamic Properties of Multiple Phases*; Weir, R. D., de Loos, T. W., Eds.; Elsevier: Amsterdam, 2005; pp 359−381.

(16) MacFarlane, D. R.; Forsyth, S. A.; Golding, J.; Deacon, G. B. Ionic liquids based on imidazolium, ammonium and pyrrolidinium salts of the dicyanamide anion. *Green Chem.* **2002**, *4*, 444–448.

(17) Deng, M. J.; Chen, P. Y.; Leong, T. I.; Sun, I. W.; Chang, J. K.; Tsai, W. T. Dicyanamide anion based ionic liquids for electrodeposition of metals. *Electrochem. Commun.* **2008**, *10*, 213–216.

(18) Chambreau, S. D.; Schneider, S.; Rosander, M.; Hawkins, T.; Gallegos, C. J.; Pastewait, M. F.; Vaghjiani, G. L. Fourier transform infrared studies in hypergolic ignition of ionic liquids. *J. Phys. Chem. A* **2008**, *112*, 7816–7824.

(19) Sobota, M.; Dohnal, V.; Vrbka, P. Activity Coefficients at Infinite Dilution of Organic Solutes in the Ionic Liquid 1-Ethyl-3-methyl-imidazolium Nitrate. *J. Phys. Chem. B* **2009**, *113*, 4323–4332.

(20) Blahut, A.; Sobota, M.; Dohnal, V.; Vrbka, P. Activity coefficients at infinite dilution of organic solutes in the ionic liquid 1-ethyl-3-methylimidazolium methanesulfonate. *Fluid Phase Equilib.* **2010**, *299*, 198–206.

(21) Blahut, A.; Dohnal, V.; Vrbka, P. Interactions of volatile organic compounds with the ionic liquid 1-ethyl-3-methylimidazolium tetracyanoborate. *J. Chem. Thermodyn.* **2011**, DOI: 10.1016/j.jct.2011.09.028.

(22) Conder, J. R.; Young, C. L. *Physicochemical Measurements by Gas Chromatography*; Wiley: New York, 1979.

(23) Víška, J.; Kiss, F. Inerton - a new support for gas chromatography. *J. Chromatogr.* **1974**, *91*, 333–345.

(24) Sanchez, L. G.; Espel, J. R.; Onink, F.; Meindersma, G. W.; De Haan, A. B. Density, Viscosity, and Surface Tension of Synthesis Grade Imidazolium, Pyridinium, and Pyrrolidinium Based Room Temperature Ionic Liquids. *J. Chem. Eng. Data* **2009**, *54*, 2803–2812.

(25) MERCK Ionic Liquid Brochure. *Electrochemistry*; Merck: Whitehouse Station, NJ, May 2011.

(26) McHale, G.; Hardacre, C.; Ge, R.; Doy, N.; Allen, R. W. K.; MacInnes, J. M.; Bown, M. R.; Newton, M. I. Density-viscosity product of small-volume ionic liquid samples using quartz crystal impedance analysis. *Anal. Chem.* **2008**, *80*, 5806–5811.

(27) Abraham, M. H. Scales of Solute Hydrogen-bonding: Their Construction and Application to Physicochemical and Biochemical Processes. *Chem. Soc. Rev.* **1993**, *22*, 73–83.

(28) Abraham, M. H.; Ibrahim, A. M.; Zissimos, J. Determination of sets of solute descriptors from chromatographic measurements. *J. Chromatogr., A* **2004**, *1037*, 29–47.

(29) Poole, S. K.; Poole, C. F. Chemometric classification of the solvent properties (selectivity) of commonly used gas chromatographic stationary phases. *J. Chromatogr., A* **1995**, *697*, 415–427.

(30) Poole, C. F.; Poole, S. K. Column selectivity from the perspective of the solvation parameter model. *J. Chromatogr., A* **2002**, *965*, 263–299.

(31) Acree, W. E.; Abraham, M. H. The analysis of solvation in ionic liquids and organic solvents using the Abraham linear free energy relationship. *J. Chem. Technol. Biotechnol.* **2006**, *81*, 1441–1446.

(32) Abraham, M. H.; Acree, W. E. Comparative analysis of solvation and selectivity in room temperature ionic liquids using the Abraham linear free energy relationship. *Green Chem.* **2006**, *8*, 906–915.

(33) Sprunger, L. M.; Proctor, A.; Acree, W. E., Jr.; Abraham, M. H. LFER correlations for room temperature ionic liquids: Separation of equation coefficients into individual cation-specific and anion-specific contributions. *Fluid Phase Equilib.* **2008**, *265*, 104–111.

(34) Abraham, M. H.; Ibrahim, A. M.; Acree, W. E., Jr. Partition of compounds from gas to water and from gas to physiological saline at 310 K: Linear free energy relationships. *Fluid Phase Equilib.* **2007**, *251*, 93–109.

(35) Fumino, K.; Wulf, A.; Verevkin, S. P.; Heintz, A.; Ludwig, R. Estimating Enthalpies of Vaporization of Imidazolium-Based Ionic Liquids from Far-Infrared Measurements. *ChemPhysChem* **2010**, *11*, 1623–1626.

(36) Deyko, A.; Lovelock, K. R. J.; Corfield, J. A.; Taylor, A. W.; Gooden, P. N.; Villar-Garcia, I. J.; Licence, P.; Jones, R. G.; Krasovskiy, V. G.; Chernikova, E. A.; et al. Measuring and predicting ΔH-vap(298) values of ionic liquids. *Phys. Chem. Chem. Phys.* **2009**, *11*, 8544–8555.

(37) Emel'yanenko, V. N.; Verevkin, S. P.; Heintz, A.; Schick, C. Ionic Liquids. Combination of Combustion Calorimetry with High-Level Quantum Chemical Calculations for Deriving Vaporization Enthalpies. *J. Phys. Chem. B* **2008**, *112*, 8095–8098.

(38) Domanska, U.; Marciniak, A. Measurements of activity coefficients at infinite dilution of aromatic and aliphatic hydrocarbons, alcohols, and water in the new ionic liquid [EMIM][SCN] using GLC. *J. Chem. Thermodyn.* **2008**, *40*, 860–866.

(39) Domanska, U.; Krolikowska, M. Measurements of Activity Coefficients at Infinite Dilution in Solvent Mixtures with Thiocyanate-Based Ionic Liquids Using GLC Technique. *J. Phys. Chem. B* **2010**, *114*, 8460–8466.

(40) Mutelet, F.; Revelli, A. L.; Jaubert, J. N.; Sprunger, L. M.; Acree, W. E.; Baker, G. A. Partition Coefficients of Organic Compounds in New Imidazolium and Tetralkylammonium Based Ionic Liquids Using Inverse Gas Chromatography. *J. Chem. Eng. Data* **2010**, *55*, 234–242.

(41) Domanska, U.; Redhi, G. G.; Marciniak, A. Activity coefficients at infinite dilution measurements for organic solutes and water in the ionic liquid 1-butyl-1-methylpyrrolidinium trifluoromethanesulfonate using GLC. *Fluid Phase Equilib.* **2009**, *278*, 97–102.

(42) Kato, R.; Gmehling, J. Systems with ionic liquids: Measurement of VLE and $\gamma(\infty)$ data and prediction of their thermodynamic behavior using original UNIFAC, mod. UNIFAC(Do) and COSMO-RS(O1). *J. Chem. Thermodyn.* **2005**, *37*, 603–619.

(43) Domanska, U.; Krolikowski, M.; Acree, W. E. Thermodynamics and activity coefficients at infinite dilution measurements for organic solutes and water in the ionic liquid 1-butyl-1-methylpyrrolidinium tetracyanoborate. *J. Chem. Thermodyn.* **2011**, DOI: 10.1016/j.jct.2011.06.007.

(44) *PLACID - Prague Limiting Activity Coefficient Inquiry Database*; Department of Physical Chemistry, Institute of Chemical Technology: Prague, 1999.

(45) Goral, M.; Kolasinska, G.; Oracz, P.; Warycha, S. Vapor-Liquid Equilibria. II. The Ternary System Methanol-Chloroform-Acetone at 313.15 and 323.15 K. *Fluid Phase Equilib.* **1985**, *23*, 89–116.

(46) Yan, W. D.; Rose, C.; Gmehling, J. Isothermal vapor-liquid equilibrium data for the ethanol plus ethyl acetate plus sodium iodide system at five temperatures. *J. Chem. Eng. Data* **1997**, *42*, 603–608.